RESEARCH ARTICLE | MAY 08 2024

# Producing two-dimensional dust clouds and clusters using a movable electrode for complex plasma and fundamental physics experiments *⊙*

Ravi Kumar <sup>(1)</sup>; Zhibo Liu <sup>(1)</sup>; Saikat Chakraborty Thakur <sup>(1)</sup>; Edward Thomas, Jr. <sup>(1)</sup>; Ranganathan Gopalakrishnan **∑** <sup>(1)</sup>



Rev. Sci. Instrum. 95, 053503 (2024) https://doi.org/10.1063/5.0203259





# Articles You May Be Interested In

Dust vortex flow analysis in weakly magnetized plasma

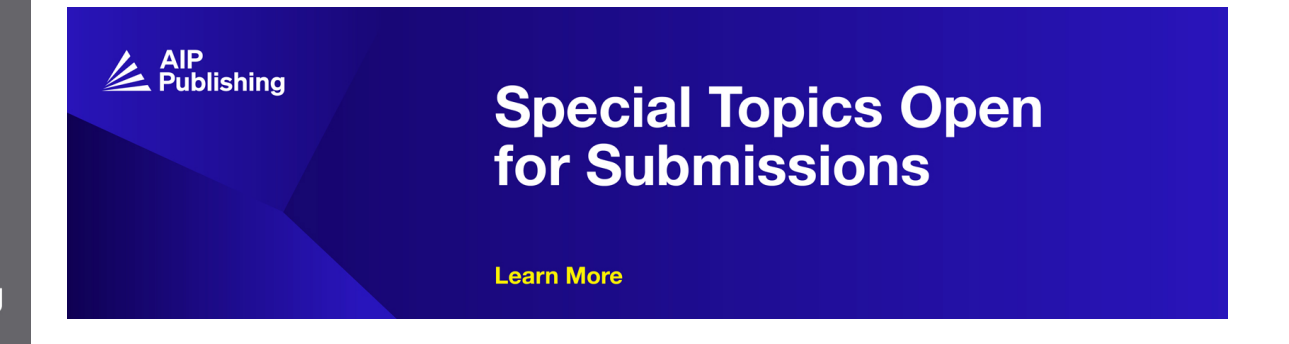
Phys. Plasmas (June 2020)

Design and characterization of a movable emittance meter for low-energy electron beams

Rev. Sci. Instrum. (September 2006)

Ultrahigh vacuum scanning electron microscope system combined with wide-movable scanning tunneling microscope

Rev. Sci. Instrum. (August 2005)





# Producing two-dimensional dust clouds and clusters using a movable electrode for complex plasma and fundamental physics experiments

Cite as: Rev. Sci. Instrum. 95, 053503 (2024); doi: 10.1063/5.0203259

Submitted: 12 February 2024 • Accepted: 22 April 2024 •

Published Online: 8 May 2024







Ravi Kumar,<sup>1</sup> D Zhibo Liu,<sup>1</sup> Saikat Chakraborty Thakur,<sup>2</sup> D Edward Thomas, Jr.,<sup>2</sup> D and Ranganathan Gopalakrishnan<sup>1,a)</sup>

#### **AFFILIATIONS**

- Department of Mechanical Engineering, University of Memphis, Memphis, Tennessee 38152, USA
- <sup>2</sup>Physics Department, Auburn University, Auburn, Alabama 36832, USA

#### **ABSTRACT**

We report a Bidirectional Electrode Control Arm Assembly (BECAA) for precisely manipulating dust clouds levitated above the powered electrode in RF plasmas. The reported techniques allow the creation of perfectly 2D dust layers by eliminating off-plane particles by moving the electrode from outside the plasma chamber without altering the plasma conditions. The tilting and moving of electrodes using BECAA also allows the precise and repeatable elimination of dust particles one by one to achieve any desired number of grains N without trial and error. Simultaneously acquired top and side view images of dust clusters show that they are perfectly planar or 2D. A demonstration of clusters with N=1-28 without changing the plasma conditions is presented to show the utility of BECAA for complex plasma and statistical physics experimental design. Demonstration videos and 3D printable part files are available for easy reproduction and adaptation of this new method to repeatably produce 2D clusters in existing RF plasma chambers.

Published under an exclusive license by AIP Publishing. https://doi.org/10.1063/5.0203259

### I. INTRODUCTION

Complex plasmas (gas discharges containing dust grains) are classical analogs or test beds of real matter. Laboratory complex plasma experiments involving the introduction of well-characterized microparticles amenable for optical tracking have been numerously used to probe grain collective phenomena such as dustacoustic waves, <sup>1–5</sup> structural phase transitions, <sup>6–12</sup> thermal energy transport, <sup>13–15</sup> viscous <sup>16–20</sup> and visco-elastic <sup>21,22</sup> dissipation, and properties of crystal lattices. <sup>23–29</sup> Observed grain trajectories have also been used to infer the electric charge and ion drag force on individual grains. <sup>30–39</sup> The motivations for understanding the collective behavior of charged grains in plasmas originate from stellar and planetary astrophysics, <sup>40–44</sup> plasma-based materials processing and semiconductor manufacturing, <sup>45–50</sup> nuclear fusion devices, <sup>51–53</sup> and space exploration, <sup>54</sup> to name a few.

A key step in a complex plasma experiment is the introduction of dust into the plasma, typically produced as an RF glow discharge.

The charge carriers in plasmas produced from the ionization of noble gases (Ar, Ne, He, etc.) are generally singly charged positive ions (Ar<sup>+</sup>, Ne<sup>+</sup>, He<sup>+</sup>, etc.) and electrons ( $e^-$ ). Consequently, individual dust grains acquire a negative potential (in ~  $\mu$ s timescales) and levitate above the electrode. Under conditions of earthly gravity, the weight of charged grains  $\vec{F}_G$  is balanced by the strong electric field  $\vec{E}_{sh}$  that exists in the sheath region above the powered/biased electrode. Grains of the same size levitate in the same plane, leading to a two-dimensional (2D) cluster/cloud whose radial extent and structure are determined by a force balance on the grains [Fig. 1(a)] that includes

- grain-grain mutual repulsion determined by their electric charge,
- ion drag force  $\vec{F}_{id}$  due to axial and radial ion flows over the grains, and
- radial confinement due to an annular step at the edge of the circular electrode  $\vec{F}_{conf}$ .

a) Author to whom correspondence should be addressed: rgplkrsh@memphis.edu

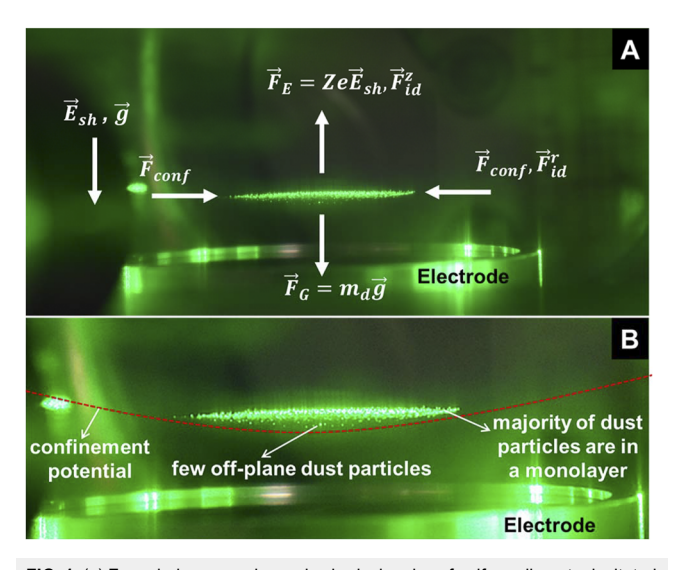


**FIG. 1.** (a) Force balance on charged spherical grains of uniform diameter levitated above the powered electrode.  $\vec{E}_{sh}$  is the sheath electric field;  $\vec{g}$  is the vertical direction where gravity acts;  $\vec{F}_{conf}$  is the radial confinement force due to an annular step at the edge of the circular electrode; Z is the grain charge;  $m_d$  is the grain mass;  $F_{id}^2$  and  $F_{id}^r$ , respectively, are the axial and radial components of the ion drag force  $\vec{F}_{id}$ ; and neutral drag force is not depicted here due to the absence of any bulk gas flows or significant drift over the electrode. (b) Overlap of a parabolic confinement potential that traps grains in a quasi-2D layer.

Numerous complex plasma experimental studies, since the discovery of dusty or complex plasmas in the laboratory, have created 2D dust clouds in RF discharges for trajectory analysis and statistical investigations. Despite the simplicity of dropping powders consisting of monodisperse dust grains and letting the grains find their equilibrium positions, formed 2D layers almost always tend to have a few off-plane grains that render them only quasi-2D as shown in Fig. 1(b). The off-plane grains are the result of asymmetric shielding of grain charge by the plasma ions at different heights along the plasma chamber axis due to the axial streaming of ions toward the bottom-powered electrode. To minimize the number of off-plane particles, trial-and-error, that is, repeating the experiment by re-injecting the monodispersed dust grains until they form a desired two-dimensional monolayer, is employed conventionally. While perfect 2D layers would be ideal for theoretical or computational modeling, quasi-2D layers are accepted in practice as they are nevertheless useful in revealing the physics sought in a particular experiment. In this work, we describe a novel electrode assembly design called BECAA (Bidirectional Electrode Control Arm Assembly) to eliminate off-plane particles efficiently and produce truly 2D grain clusters/clouds, as verified by imaging the cloud from the side

2D clusters of charged grains containing a finite number of grains are ideal for testing statistical physics theories and predictions. The number of grains N in the cluster has been varied systematically to *computationally* probe the structure of classical many-particle systems or coulombically coupled clusters  $^{55-58}$  that are mesoscopic models of classical 2D atoms,  $^{59-62}$  ion traps  $^{63}$  used

to understand coherence and decoherence as it relates to quantum computing systems, used to visualize phase behavior  $^{64-67}$  and phase transitions  $^{68-72}$  and study the influence of defects in small clusters  $^{73-76}$  and binary mixtures.  $^{77}$  Systematically creating dust clusters with the ability to select a specific value for N in experiments is desirable to test computational predictions of the structure and phase transitions of charged particles in 2D systems.  $^{78}$ 

Several experimental studies have been reported on the shell structure of finite dust clusters in complex plasmas, <sup>79–82</sup> modal analyses of dust trajectories to quantitatively extract grain charge, interaction forces, and plasma parameters. <sup>83–86</sup> Finite clusters have also been used as a probe of the grain–grain interaction force as well as the presheath electric field. <sup>87</sup> Wolter and Melzer <sup>88</sup> have used laser to melt finite clusters to understand crystal as well as liquid states of grain motion. Detailed statistical and thermodynamic properties have been extracted from dust trajectories. <sup>89</sup> Mukhopadhyay and Goree <sup>90</sup> report experimentally measured two-particle distribution and pair correlation function. The effect of magnetic field on grain dynamics has been investigated as well. <sup>91–97</sup> In large clusters or clouds, heterogeneities in the structure have been observed. <sup>98</sup>

Recently, Singh *et al.*<sup>99</sup> have introduced radial confinement of grains using an electrified ring and used the same to induce structural transitions in the dust cloud by varying the ring voltage. This method allows the manipulation of grain structure without changing discharge conditions. Similarly, Li *et al.*<sup>100</sup> have used the striped electrode technique to control dust transport. By modulating the voltages on each electrode, they were able to manipulate and remove dust particles and to precisely manipulate the sheath structure above the powered electrode. Precise manipulation and removal of dust particles are extremely challenging in experiments. Desired clusters with a specific number of dust particles and stable plasma conditions are crucial for an accurate thermodynamic or statistical analysis.

In this article, we intend to provide a novel mechanical route to manipulate and control the density and dimensionality of the dust clouds without perturbing any electrostatic and plasma parameters of the experiment. To the best of our literature review, prior complex plasma experiments controlled charged dust grains via electromagnetic fields, which modifies the plasma conditions or disperses a desired number of grains (N) by repeated trials until the targeted N is achieved. This is especially tedious when trying to produce clusters that have a small number of grains ( $< \sim 50$ ) and do not offer the flexibility to target a specific value of N. In addition to producing a perfectly 2D dust layer, BECAA described here also allows varying N in increments of +1, leading to the systematic creation of clusters from N = 1 onward to any higher value of N with relative ease without the need for brute force trial and error. BECAA can be controlled externally (from outside of the plasma chamber) by two control arms, resulting in the creation of the N-clusters without any change in plasma parameters and experimental conditions. The systematic production of Coulombic clusters in complex/dusty plasmas with charged grains using the described electrode arm is analogous to the tunable creation of ion clusters in ion traps. 101 The rest of this article is organized as follows: the electrode arm design and working are described in Sec. II. Following that, we present images and analysis of experimentally realized dust clusters with N = 1-28 along with calculations of the grain-grain potential energy of the produced clusters in Sec. III. Finally, we summarize our conclusions in Sec. IV,

along with suggestions for potential applications of the electrode arm assembly. Live experiment videos of manipulating dust grains using control arms and 3D printable files to fabricate BECAA are provided in the supplementary material.

#### II. METHODS

The *N*-clusters were produced in the 3DPX (3D Dusty Plasma Experiment) device at the U.S. Department of Energy-funded Collaborative Research Facility Magnetized Plasma Research Laboratory, Auburn University. 3DPX consists of a six-way vacuum chamber with four transparent windows to illuminate the dust grains suspended in the plasma and two multi-port solid windows embodying the electrode assembly (BECAA), dust shaker, and probe diagnostics, as illustrated in Fig. 2. A capacitively coupled RF (13.56 MHz) discharge in argon gas was operated at 11.7 mTorr pressure and RF power of 2 W. The plasma was generated by supplying RF power to the circular electrode while keeping the vacuum chamber grounded. As the operation of BECAA does not depend on gas pressure or RF power, 2D monolayers, and finite clusters with any desired *N* can be produced for laboratory complex plasma experiments.

A circular disk-shaped metallic electrode was fabricated with a 1 mm annular step/barrier around the circumference, as shown in the inset of Fig. 2. The annular step generates a parabolic potential above the electrode to radially confine the negatively charged and mutually repulsive dust grains. Mono-sized melamine formaldehyde (MF) microspheres of diameter 6.17  $\mu$ m were used to create the dust clouds in this study. A compact 3D-printed dust shaker with a reservoir in the body and two pinholes in the cap was used to store and dispense a desired amount of dust into the plasma (Fig. 3). The amount of dust falling from the dust shaker is very crucial to producing 2D dust clouds because an excess number of dust grains that fall

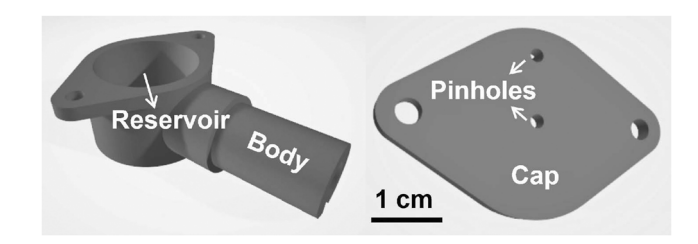


FIG. 3. Dust shaker (3D printable file included in the supplementary material).

and settle on the electrode surface could lead to a non-uniform confinement potential, adversely affecting the dynamics and uniformity of the levitated dust cloud. Once the dust grains are dispensed into the chamber, they become highly negatively charged  $(Z \sim -10^4)$ almost instantly and fall toward the bottom electrode due to gravitational force  $(\vec{F}_G = m_d \vec{g})$ , until their weight is counteracted by an upward electrostatic force  $(\vec{F}_E = Ze\vec{E}_{sh})$ , by a downward electric field originating from the RF plasma sheath above the electrode. As a result, dust grains levitate at the equilibrium position at which the downward gravitational force  $\vec{F}_G$  and upward electrostatic force  $\vec{F}_E$ are in balance [Fig. 1(a)]. A green laser of wavelength 532 nm and power 220 mW was fed through an absorptive neutral density (ND) filter of OD 0.7 (transmittance 20%), which decreased the power to ~44 mW. Then, a cylindrical lens was used to convert the laser beam of dimensions  $2.1 \times 2.5 \text{ mm}^2$  into a horizontal sheet of dimensions  $65 \times 3 \text{ mm}^2$  for homogeneous illumination of the entire dust cloud in the horizontal (x-y) plane. Similarly, a second laser of identical specifications and similar optics was used to illuminate the dust cloud vertically to visualize off-plane (z-axis) grain motion, which is shown in Fig. 2.

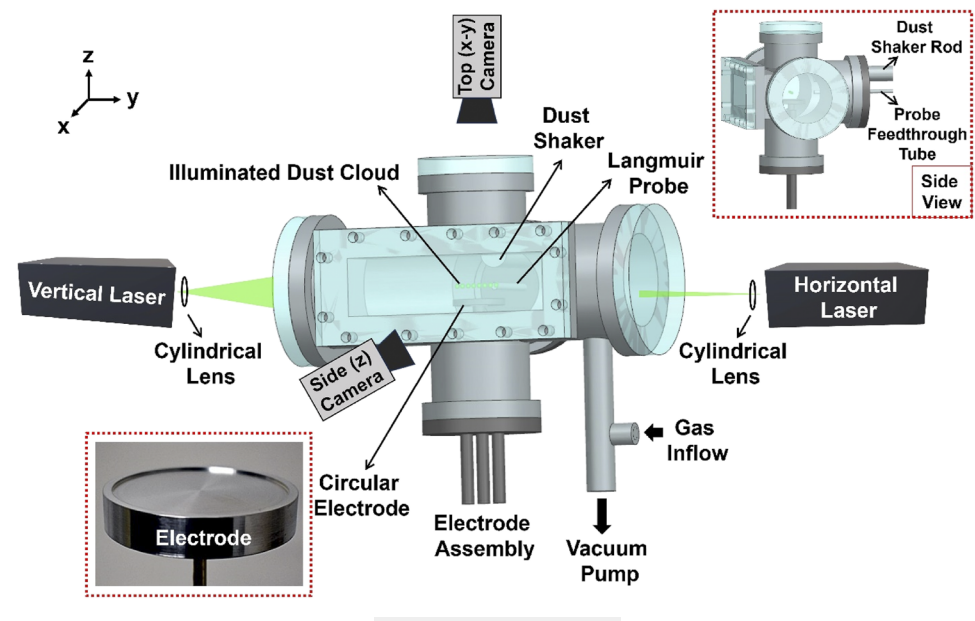
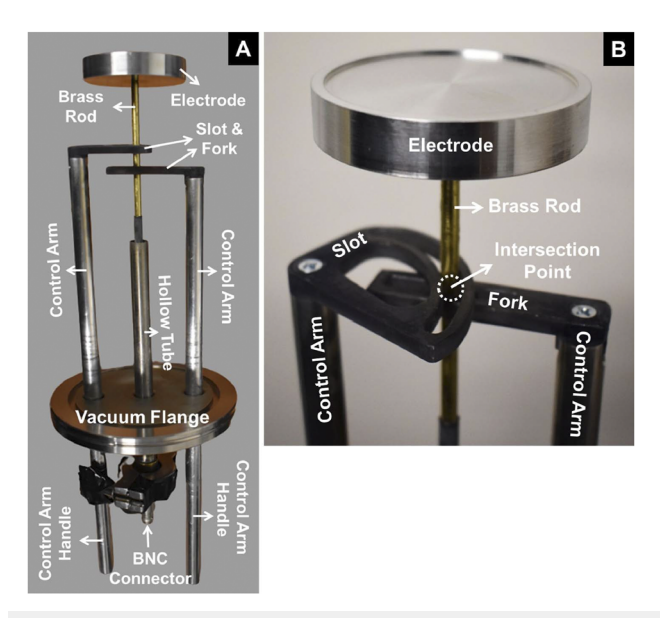


FIG. 2. 3DPX plasma device.



**FIG. 4.** (a) BECAA attached to a flange with a feedthrough for the electrode. (b) Slot and fork mechanism to move and tilt the electrode while inside a sealed vacuum chamber (3D printable files of slot and fork included in the supplementary material).

Now, the challenge is to eliminate off-plane particles to produce a perfect 2D dust monolayer. In such scenarios, the general approach in prior dusty plasma experiments is to re-inject the dust grains and anticipate that they settle in a single layer due to their

mono-sized distribution. Another common approach is to excite the whole dust cloud vertically (along the *z*-axis) by perturbing the plasma sheath using high-power pulses, forcing dust grains into a single layer or to fall onto the bottom electrode. These methods rely on multiple trials and lack repeatability, so obtaining a 2D layer without off-plane particles is not guaranteed. Lack of standardization hinders experimental design while studying the properties of finite-sized clouds or for designing well-controlled statistical physics experiments.

Bidirectional Electrode Control Arms Assembly (BECAA) is introduced as a systematic route for producing 2D dust clouds and clusters containing a finite and selectable number of grains. BECAA consists of a circular metal electrode connected with a 4 mm solid brass rod fed through a hollow vacuum tube to a BNC connector, completing the circuit for plasma generation [Fig. 4(a)]. The two adjacent control arms are installed with 3D printed fixtures "slot" and "fork" on the top, as shown in Figs. 4(a) and 4(b), and their intersection holds the central segment, while the control arm rods extend outside the vacuum chamber to be operated by a user with their handles. In this configuration, the rotational motion of the control arm handle resulted in the translation motion of the intersection point in a plane parallel to the electrode. As the other end of the brass rod is fixed in the BNC connector, the translation motion of the intersection point causes a tilt in the electrode surface. The tilt allows the removal of unwanted off-plane particles from the dust cloud. This slight tilt in the electrode assembly while the slot and fork remain stationary causes the confinement equipotential line to lower at the tilted end; thus, the negatively charged repulsive dust grains start moving toward the lowered potential region, eventually exiting from the RF plasma sheath over the electrode as shown in Figs. 5(a) and 5(b). While tilting, the perpendicular component of

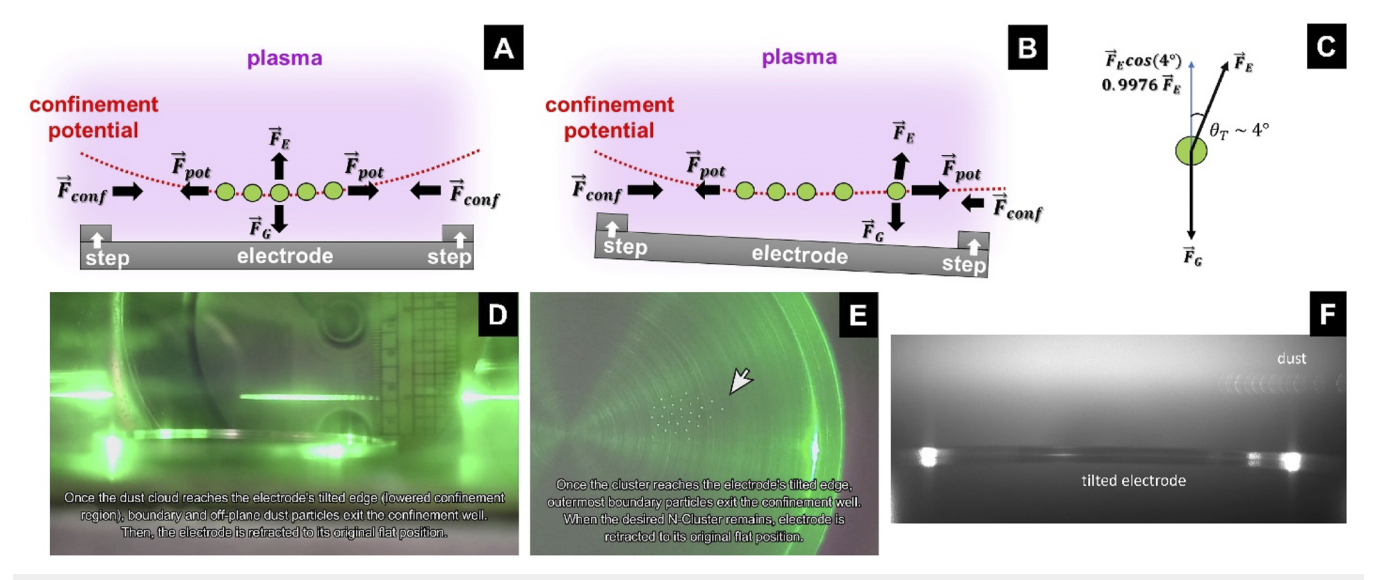


FIG. 5. (a) Force balance on dust grains in a confinement potential. (b) Force balance and motion of dust grains due to tilted electrode. (c) Vertical (z-axis) force balance on a dust grain while the electrode is titled. (d) Snapshot from demonstration videos accompanying this figure that shows the removal of multiple grains from a cloud using BECAA (Multimedia available online). (e) Snapshot from demonstration videos accompanying this figure that shows the removal of a single grain from a cluster using BECAA (Multimedia available online). (f) z-cam view of a tilted electrode and removal of grains one by one by tilting the electrode using BECAA (Multimedia available online).

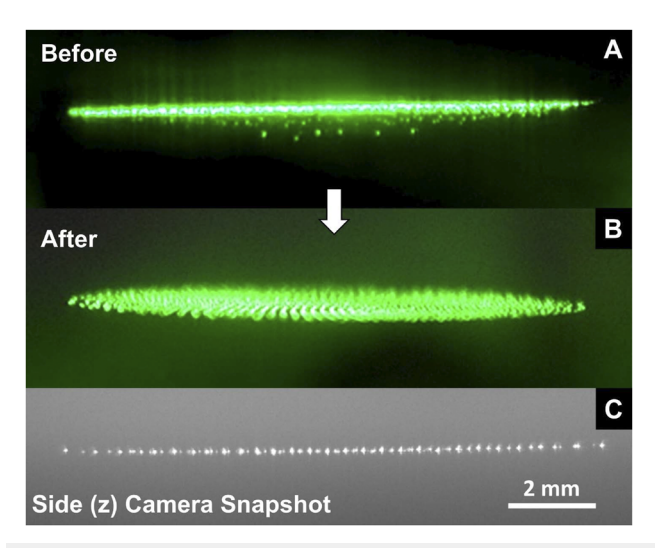
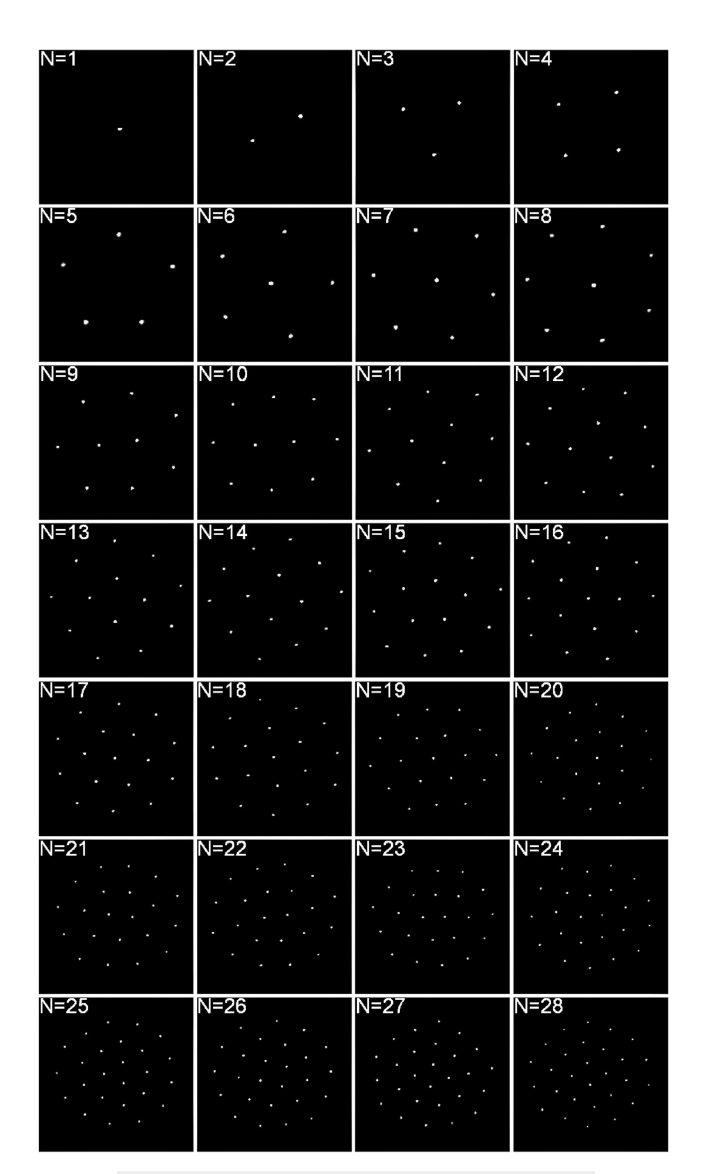


FIG. 6. [(a) and (b)] Transition from quasi-2D to 2D dust cloud. (c) Side (z) camera view with a vertical laser shining through the dust cloud.

 $\vec{F}_E$ , that is,  $\vec{F}_E \cos(\theta_T)$ , remains almost identical to the magnitude of  $\vec{F}_E$  before tilt, as the angle of tilt at which particles start radially exiting the sheath region is between  $2^{\circ}$  and  $4^{\circ}$  ( $2^{\circ} \le \theta_T \le 4^{\circ}$ ) as shown in Fig. 5(c). We used the z-axis (side view) camera to determine the tilt angle by superposing the two images, one at flat position  $(0^{\circ})$  and another at maximum tilt  $(\theta_T)$ , by which all grains exit the confinement region. Visual demonstrations of the electrode tilting and elimination of grains can be seen in Figs. 5(d)-5(f) (Multimedia available online). The maximum tilt angle was determined to be  $\theta_T \sim 4^{\circ}$ , resulting in the vertical component as  $|\vec{F}_E| \cos(\theta_T)$  $\geq 0.9976 |\vec{F}_{E}|.$  Thus,  $\vec{F}_{pot}$  (the grain–grain force), which is always a repulsive and lowered confinement force  $\vec{F}_{conf}$  in the region at the tilted edge, contributes to eliminating the grains from the sheath region above the electrode. The tilt angle can be precisely controlled using the BECAA assembly handle that extends outside the plasma chamber. This enables the manipulation of the confinement potential well shape without altering the plasma parameters or any inserted probes for diagnostics. The number of dust particles removed from the cloud is directly controlled by the degree of tilt, which determines the lowering of the confinement well shape. Therefore, multiple off-plane particles [Fig. 6(a)] can be removed simultaneously to quickly produce a perfect 2D monolayer [Fig. 6(b)]. BECAA is attached to the chamber wall, rendering it stable once set in a position and easy to operate from outside the chamber. In addition to eliminating off-plane particles, BECAA can also be used to systematically remove grains one at a time to produce finite-sized 2D dust clusters (or 2D N-clusters for brevity), where N could be as small as 1 and up to  $\sim$ 1000s of grains. For this study, we started with N = 28 and ejected grains one by one until we obtained an N = 1 cluster (Fig. 7). By keeping track of the number of grains removed, a 2D N-cluster of the desired N can be easily obtained. The dust grains were tracked through two coupled monochrome CMOS cameras, recording at 120 fps. The coupling of the top (x-y) and



**FIG. 7.** 2D clusters with N = 1-28 produced using BECAA.

side (z) cameras was necessary to simultaneously visualize the dust motion in horizontal and vertical planes and confirm that there are no off-plane particles in the dust cloud [Figs. 6(c) and 8]. While most of our clusters were in a crystal-like state of organization, in those that exhibit fluid-like behavior, the z-axis camera can also be used to obtain their off-plane motion quantitatively.

## III. RESULTS AND DISCUSSION

Figure 7 displays the high-resolution images of the clusters we obtained for N=1-28 in the RF discharge operated at 2 W power and 11.7 mTorr Ar gas pressure. Under these conditions, the electric charge on each grain is estimated as  $Z \approx -14\,000e$  by solving  $I_e = I_i$ . Here,  $I_e$  is the collisionless electron current to the grain

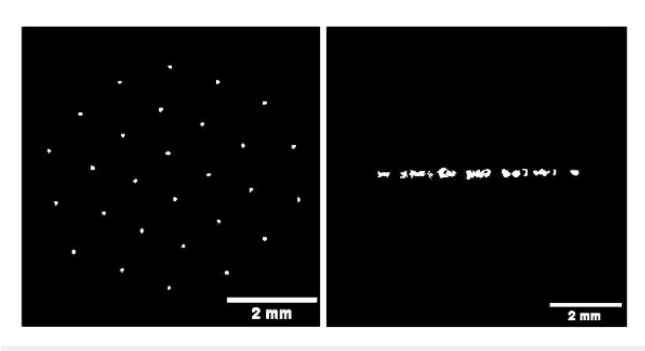


**FIG. 8.** Top view (left panel) and side view (right panel) of a cluster that confirm that all grains are in the same plane.

calculated using OML theory,  $^{102,103}$  and  $I_i$  is the collisional ion current calculated using the experimentally validated model by Suresh et al. 104 The plasma Debye length  $\lambda_D$  is estimated using the velocitydependent shielding length expression by Hutchinson and Khrapak <sup>06</sup> as 269  $\mu$ m, assuming  $u_i \cong v_B$  ( $u_i$  is the ion velocity and  $v_B$  is the Bohm velocity) as dust levitates at the sheath boundary. Electron concentration  $n_e \sim 9 \times 10^{14} \text{ m}^{-3}$  and electron temperature  $T_e \sim 3.5$  eV were obtained via Langmuir probe measurements. From the velocity distributions of the grains, it was evident that the produced clusters are in a crystal-like or solid-like state as the kinetic energy of individual grains is much smaller than the cluster electrostatic potential energy. The cluster energy is calculated as the sum of the pairwise electrostatic potential energy of the grains without including their kinetic energies and their potential energy due to their position in the confinement well:  $E(N) \cong \frac{Z^2 e^2}{4\pi e_0} \sum_{i=1}^{N-1} \sum_{j=i+1}^{N} \frac{1}{r_{ij}} e^{-\frac{r_{ij}}{\lambda_D}}. \frac{E(N)}{N}$  in J is displayed in Table I for the experimentally obtained N-clusters along with the nondimensional  $\frac{E}{N}$  obtained using Monte Carlo simulations by Bedanov and Peeters.<sup>78</sup> Table I is presented as a demonstration of obtaining clusters without gaps in the N for scientific experimentation. The cluster energy analysis by Bedanov and Peeters<sup>78</sup> is experimentally realized here using the described BECAA without gaps in N. Quantitative comparison would be possible by including experiment-specific details in the simulations. Since the structures can be created with a prescribed *N*, other thermodynamic quantities, especially structural entropy,107 can be computed based on experimental data. The experimental routine involved starting with a large cloud that included a few off-plane grains [such as in Fig. 1(b)], which were removed by tilting the electrode. Next, the grains were removed from the cloud, initially in tens and then later one by one, until the desired number of grains was attained. We started with N = 28 grains and eliminated them one by one to obtain the clusters shown in Fig. 7. The side view presented in Fig. 8 confirms that all the grains are in the same plane, and BECAA leads to purely 2D clusters. We construe this as a systematic demonstration of the ability of BECAA to obtain the desired clusters for fundamental physics experiments. The key advance is the elimination of trial and error and the need for changing plasma parameters while trying to produce clusters of desired N. Peeters, Schweigert, and Bedanov<sup>60</sup> developed a Mendeleev-type periodic table for classical 2D atoms (clusters) and also for molecules, <sup>59,108</sup> in which the

**TABLE I.** Calculations of average grain–grain potential energy  $\frac{E}{N}$  for the clusters experimentally obtained using BECAA along with modeling calculations of Bedanov and Peeters. <sup>78</sup> The key advantage of using BECAA is the ability to obtain clusters without any gaps in *N*. Plasma discharge conditions are 2 W and 11.7 mTorr.

Cluster size N	Average grain–grain potential energy per grain $\frac{E}{N}$ (×10 <sup>-19</sup> J)	Non-dimensional $\frac{E}{N}$ from Bedanov and Peeters <sup>78</sup>
1	0	0
2	1.67	0.75
3	1.94	1.310 37
4	2.67	1.835 45
5	3.81	2.338 45
6	4.21	2.804 56
7	4.44	3.238 97
8	5.38	3.668 9
9	6.11	4.088 13
10	6.71	4.484 94
11	7.35	4.864 67
12	8.65	5.238 95
13	8.62	5.601 14
14	9.35	5.958 99
15	10.6	6.307 58
16	11.1	6.649 9
17	10.3	6.982 91
18	10.9	7.308 14
19	11.6	7.631 97
20	12.0	7.949 61
21	12.4	8.265 88
22	12.7	8.574 18
23	13.2	8.877 65
24	14.9	9.175 9
25	15.8	9.470 79
26	16.3	9.762 73
27	20.4	10.0509
28	16.8	10.335 6

Hamiltonian for the clusters was taken as the sum of the pairwise grain–grain Coulombic potential energy  $\sum_{i=1}^{N-1}\sum_{j=i+1}^{N}\varphi_{ij}$  and the potential energy due to position in the confinement well  $\sum_{i=1}^{N} V(\vec{r_i})$ . Using BECAA, such theoretical predictions can now be verified and demonstrated with relative ease. Juan et al. 79 approximated linear chains with 5-20 grains as quasi-2D clusters (when viewed from the top) and conducted structural analysis. This experiment could now be potentially done without gaps in N using BECAA and the analysis be done exactly without simplifying assumptions. Experiments such as those by Schella et al.89 were done to understand the thermodynamic behavior of clusters as a function of N. Only selected N = 19, 20, 27, 34 were used, potentially due to challenges in systematically producing clusters from N = 1 to any desired N. BECAA enables experimental design that is closely knit with computational modeling. Probing the effect of an externally applied magnetic field on the dynamics of  $\mu$ m-sized grains dispersed in a plasma continues to garner growing interest. 91-97 BECAA allows systematic experimental design without changing the RF discharge parameters, as

demonstrated in the clusters displayed in Table I. Video demonstrations of manipulating dust grains using BECAA and 3D printable files of the compact dust shaker and BECAA components "slot" and "fork" are provided in the supplementary material for quick and convenient integration of such an electrode assembly into dusty or complex plasma experimental investigations.

#### IV. CONCLUSIONS

The presented design of the Bidirectional Electrode Control Arms Assembly (BECAA) allows the realization of truly twodimensional dust clouds or clusters above the powered electrode in RF discharges. We demonstrated the ability of BECAA to produce perfect monolayers and clusters of selectable N from nonuniform 3D or quasi-2D dust clouds, keeping plasma conditions constant throughout the experiment. We utilized vertical laser illumination and side-view imaging to show that the produced clusters do not contain any off-plane dust particles. In addition, by the methods described herein, the clusters were produced in a relatively short period of time, and the procedure is systematic and extremely repeatable. In contrast, the general trial-and-error methods fail to offer such rapidity, repeatability, and certainty to generate the desired N-cluster or a 2D monolayer. We also emphasized the importance of such controlled clusters for fundamental physics experiments relevant to many sub-disciplines, such as statistical physics, classical electrostatics, materials science, and dusty or complex plasmas. Complex plasmas created by dispersing grains are a unique experimental system to study 2D systems of classically interacting particles. To obtain insights into the behavior of 2D systems, BECAA offers greater control over experimental design and associated theoretical or numerical modeling. Control over the number of grains provided by BECAA could be potentially effective in visualizing the multi-body electrostatic interactions in classical systems. BECAA has been used in conditions where the grains organize into a crystal state in the presence of parabolic confinement. It remains to be explored how BECAA can interact with clouds that are in a fluid state. Further work on designing experiments to create small clusters to explore multi-body collisional interactions, structural transitions, and thermodynamics is of interest. This is of potential utility in modeling grain dynamics and in understanding the grain behavior in low-temperature plasmas used for a broad range of applications. 109-111 BECAA is demonstrated here in an RF discharge, and future work could potentially build versions for other types of plasma discharges as well. Finally, the presented BECAA approach advanced here could be potentially useful in dusty plasma research and as a pedagogical tool to visualize concepts such as electrostatics, collisional scattering, and stochastic dynamics.

#### SUPPLEMENTARY MATERIAL

The supplementary material contains the 3D printable files of the dust shaker as shown in Fig. 3 and the slot and fork of BECAA as shown in Fig. 4(b). The files are in .SLDPRT format that can be directly used to print using a 3D printer. The Dust Shaker folder has three printable files for each section: body (with a feedthrough attachment and a reservoir), bottom (to seal the reservoir), and cap

(to close the dust shaker and pin holes to eject the dust particles from the reservoir).

#### **ACKNOWLEDGMENTS**

Funding for this research was provided by the U.S. Department of Energy FY2020 Early Career Award No. DE-SC0021146 and Facilities Award No. DE-SC0023416 from the Office of Fusion Energy Sciences. The access to Magnetized Plasma Research Laboratory, Auburn University, was granted through a MagNetUS consortium allocation. The authors thank Mr. Cameron Royer from MPRL for his assistance.

#### **AUTHOR DECLARATIONS**

#### **Conflict of Interest**

The authors have no conflicts to disclose.

#### **Author Contributions**

Ravi Kumar: Conceptualization (lead); Data curation (lead); Formal analysis (lead); Investigation (equal); Methodology (equal); Writing – original draft (supporting); Writing – review & editing (supporting). Zhibo Liu: Conceptualization (equal); Investigation (supporting); Methodology (equal). Saikat Thakur: Investigation (supporting); Methodology (supporting); Resources (supporting); Supervision (supporting). Edward Thomas, Jr.: Funding acquisition (supporting); Investigation (supporting); Methodology (supporting); Resources (equal). Ranganathan Gopalakrishnan: Conceptualization (equal); Formal analysis (supporting); Funding acquisition (lead); Investigation (equal); Project administration (lead); Resources (lead); Supervision (lead); Writing – original draft (lead); Writing – review & editing (equal).

#### **DATA AVAILABILITY**

The data that support the findings of this study are available within the article and its supplementary material.

#### **REFERENCES**

- <sup>1</sup>V. V. Yaroshenko, S. A. Khrapak, M. Y. Pustylnik, H. M. Thomas, S. Jaiswal, A. M. Lipaev, A. D. Usachev, O. F. Petrov, and V. E. Fortov, *Phys. Plasmas* **26**, 053702 (2019).
- <sup>2</sup>S. Jaiswal, P. Bandyopadhyay, and A. Sen, Phys. Plasmas 23, 083701 (2016).
- <sup>3</sup> A. Usachev, A. Zobnin, O. Petrov, V. Fortov, M. H. Thoma, H. Hofner, M. Fink, A. Ivlev, and G. Morfill, New J. Phys. **16**, 053028 (2014).
- <sup>4</sup>V. Nosenko, S. K. Zhdanov, S. H. Kim, J. Heinrich, R. L. Merlino, and G. E. Morfill, Europhys. Lett. **88**, 65001 (2009).
- <sup>5</sup>D. Samsonov, J. Goree, Z. W. Ma, A. Bhattacharjee, H. M. Thomas, and G. E. Morfill, Phys. Rev. Lett. **83**, 3649 (1999).
- <sup>6</sup>Z. Haralson and J. Goree, IEEE Trans. Plasma Sci. 44, 549 (2016).
- <sup>7</sup> A. Schella, T. Miksch, A. Melzer, J. Schablinski, D. Block, A. Piel, H. Thomsen, P. Ludwig, and M. Bonitz, Phys. Rev. E 84, 056402 (2011).
- <sup>8</sup>Y. Feng, J. Goree, and B. Liu, Phys. Rev. Lett. **100**, 205007 (2008).
- <sup>9</sup> A. Melzer, A. Homann, and A. Piel, Phys. Rev. E **53**, 2757 (1996).
- <sup>10</sup>P. Hartmann, A. Douglass, J. C. Reyes, L. S. Matthews, T. W. Hyde, A. Kovacs, and Z. Donko, Phys. Rev. Lett. 105, 115004 (2010).

- <sup>11</sup> A. V. Ivlev, U. Konopka, G. Morfill, and G. Joyce, Phys. Rev. E 68, 026405 (2003).
- <sup>12</sup>R. A. Quinn and J. Goree, Phys. Rev. E 64, 051404 (2001).
- 13 V. E. Fortov, O. S. Vaulina, O. F. Petrov, I. A. Shakhova, A. V. Gavrikov, and Y. V. Khrustalev, Plasma Phys. Rep. 32, 323 (2006).
- <sup>14</sup>Y. Feng, J. Goree, and B. Liu, Phys. Rev. E **86**, 056403 (2012).
- <sup>15</sup>V. Nosenko, S. Zhdanov, A. V. Ivlev, G. Morfill, J. Goree, and A. Piel, Phys. Rev. Lett. 100, 025003 (2008).
- <sup>16</sup>Z. Haralson and J. Goree, Phys. Plasmas 23, 093703 (2016).
- <sup>17</sup>Y. Feng, J. Goree, B. Liu, and E. G. D. Cohen, Phys. Rev. E 84, 046412 (2011).
- <sup>18</sup>B. Liu and J. Goree, Phys. Plasmas **24**, 103702 (2017).
- <sup>19</sup> Y. Feng, J. Goree, and B. Liu, Phys. Rev. Lett. **109**, 185002 (2012).
- <sup>20</sup>Z. Donkó, J. Goree, P. Hartmann, and K. Kutasi, Phys. Rev. Lett. 96, 145003 (2006).
- <sup>21</sup> Y. Feng, J. Goree, and B. Liu, Phys. Rev. E **85**, 066402 (2012).
- <sup>22</sup>Y. Feng, J. Goree, and B. Liu, Phys. Rev. Lett. **105**, 025002 (2010).
- <sup>23</sup> M. H. Thoma, M. Kretschmer, H. Rothermel, H. M. Thomas, and G. E. Morfill, Am. J. Phys. 73, 420 (2005).
- <sup>24</sup>P. Hartmann, A. Z. Kovacs, A. M. Douglass, J. C. Reyes, L. S. Matthews, and T. W. Hyde, Phys. Rev. Lett. 113, 025002 (2014).
- <sup>25</sup>L. S. Matthews, K. Qiao, and T. W. Hyde, Adv. Space Res. 38, 2564 (2006).
- <sup>26</sup> A. Piel, V. Nosenko, and J. Goree, Phys. Rev. Lett. **89**, 085004 (2002).
- <sup>27</sup>J. B. Pieper, J. Goree, and R. A. Quinn, *Phys. Rev. E* **54**, 5636 (1996).
- <sup>28</sup> A. M. Lipaev, V. I. Molotkov, A. P. Nefedov, O. F. Petrov, V. M. Torchinskii, V. E. Fortov, A. G. Khrapak, and S. A. Khrapak, J. Exp. Theor. Phys. 85, 1110 (1997).
- <sup>29</sup>R. A. Quinn, C. Cui, J. Goree, J. B. Pieper, H. Thomas, and G. E. Morfill, Phys. Rev. E 53, R2049 (1996).
- <sup>30</sup>C. Zafiu, A. Melzer, and A. Piel, Phys. Plasmas **9**, 4794 (2002).
- <sup>31</sup>C. Zafiu, A. Melzer, and A. Piel, Phys. Plasmas 10, 1278 (2003).
- <sup>32</sup> M. Hirt, D. Block, and A. Piel, Phys. Plasmas 11, 5690 (2004).
- 33 M. Hirt, D. Block, and A. Piel, IEEE Trans. Plasma Sci. 32, 582 (2004).
- 34V. Yaroshenko, S. Ratynskaia, S. Khrapak, M. H. Thoma, M. Kretschmer, H. Höfner, G. E. Morfill, A. Zobnin, A. Usachev, O. Petrov, and V. Fortov, Phys. Plasmas 12, 093503 (2005).
- <sup>35</sup>V. V. Yaroshenko, S. Ratynskaia, S. A. Khrapak, M. H. Thoma, M. Kretschmer, and G. E. Morfill, Contrib. Plasma Phys. 45, 223 (2005).
- <sup>36</sup>V. Nosenko, R. Fisher, R. Merlino, S. Khrapak, G. Morfill, and K. Avinash, Phys. Plasmas 14, 103702 (2007).
- <sup>37</sup>J. Beckers, D. J. M. Trienekens, and G. M. W. Kroesen, Phys. Rev. E 88, 055101 (2013).
- 38 S. A. Khrapak, M. H. Thoma, M. Chaudhuri, G. E. Morfill, A. V. Zobnin, A. D. Usachev, O. F. Petrov, and V. E. Fortov, Phys. Rev. E 87, 063109 (2013).
- <sup>39</sup>T. H. Hall and E. Thomas, IEEE Trans. Plasma Sci. **44**, 463 (2016).
- <sup>40</sup>U. de Angelis, V. Formisano, and M. Giordano, J. Plasma Phys. 40, 399 (2009).
- <sup>41</sup>C. K. Goertz, Rev. Geophys. **27**, 271, https://doi.org/10.1029/rg027i002p00271
- <sup>42</sup>D. A. Mendis and M. Rosenberg, Annu. Rev. Astron. Astrophys. 32, 419 (1994).
- <sup>43</sup>M. Horányi, Annu. Rev. Astron. Astrophys. **34**, 383 (1996).
- <sup>44</sup>P. K. Shukla, *Dust Plasma Interaction in Space* (Nova Science Publishers, 2002).
- <sup>45</sup>L. Couëdel, D. Artis, M. P. Khanal, C. Pardanaud, S. Coussan, S. LeBlanc, T. Hall, E. Thomas, Jr., U. Konopka, M. Park, and C. Arnas, Plasma Res. Express 1,015012 (2019).
- <sup>46</sup>B. Tadsen, F. Greiner, and A. Piel, Phys. Plasmas 21, 103704 (2014).
- <sup>47</sup>M. Schulze, D. O'Connell, T. Gans, P. Awakowicz, and A. von Keudell, Plasma Sources Sci. Technol. 16, 774 (2007).
- <sup>48</sup>D. Samsonov et al., New J. Phys. 5, 24 (2003).
- 49 N. Sato, G. Uchida, T. Kaneko, S. Shimizu, and S. Iizuka, Phys. Plasmas 8, 1786
- 50 S. C. Yang, Y. Nakajima, Y. Maemura, Y. Matsuda, and H. Fujiyama, Plasma Sources Sci. Technol. 5, 333 (1996).

- <sup>51</sup>E. Lazzaro, I. Proverbio, F. Nespoli, S. Ratynskaia, C. Castaldo, U. deAngelis, M. DeAngeli, J. P. Banon, and L. Vignitchouk, Plasma Phys. Controlled Fusion 54, 124043 (2012).
- 52 T. Reichenstein, J. Wilms, F. Greiner, A. Piel, and A. Melzer, Contrib. Plasma Phys. 52, 813 (2012).
- <sup>53</sup>T. Reichstein, I. Pilch, and A. Piel, Phys. Plasmas 17, 093701 (2010).
- <sup>54</sup>I. D. Kaganovich, A. Smolyakov, Y. Raitses, E. Ahedo, I. G. Mikellides, B. Jorns, F. Taccogna, R. Gueroult, S. Tsikata, A. Bourdon et al., Phys. Plasmas 27, 120601
- <sup>55</sup>T. Kamimura, Y. Suga, and O. Ishihara, *Phys. Plasmas* **14**, 123706 (2007).
- <sup>56</sup>K. Nelissen, A. Matulis, B. Partoens, M. Kong, and F. M. Peeters, Phys. Rev. E 73, 016607 (2006).
- <sup>57</sup>S. G. Amiranashvili, N. G. Gusein-zade, and V. N. Tsytovich, Phys. Rev. E **64**, 016407 (2001).
- <sup>58</sup>G. Date, M. V. N. Murthy, and R. Vathsan, J. Phys.: Condens. Matter 10, 5875
- <sup>59</sup>B. Partoens and F. M. Peeters, J. Phys.: Condens. Matter **9**, 5383 (1997).
- $^{\bf 60}{\rm F.~M.}$  Peeters, V. A. Schweigert, and V. M. Bedanov, Physica B  $\bf 212,$  237 (1995).
- <sup>61</sup>S. Bednarek, B. Szafran, and J. Adamowski, Phys. Rev. B **59**, 13036 (1999).
- 62 V. A. Schweigert and F. M. Peeters, J. Phys.: Condens. Matter 10, 2417 (1998).
- <sup>63</sup>R. A. Beekman, M. R. Roussel, and P. J. Wilson, *Phys. Rev. A* **59**, 503 (1999).
- <sup>64</sup>S. W. S. Apolinario, B. Partoens, and F. M. Peeters, New J. Phys. **9**, 283 (2007). <sup>65</sup>K. Nelissen, B. Partoens, and F. M. Peeters, Phys. Rev. E **71**, 066204 (2005).
- <sup>66</sup>A. Radzvilavičius and E. Anisimovas, J. Phys.: Condens. Matter 23, 075302 (2011).
- 67 J. Cioslowski and J. Albin, J. Chem. Phys. 136, 114306 (2012).
- <sup>68</sup>S. W. S. Apolinario and F. M. Peeters, Phys. Rev. E **76**, 031107 (2007).
- <sup>69</sup>D. M. Tomecka, B. Partoens, and F. M. Peeters, Phys. Rev. E **71**, 062401 (2005).
- $^{\bf 70}{\rm F.\,M.}$  Peeters, in Two-Dimensional Electron Systems: On Helium and Other Cryogenic Substrates, edited by E. Y. Andrei (Springer Netherlands, Dordrecht, 1997), p. 17.

  71 M. Kong, B. Partoens, and F. M. Peeters, Phys. Rev. E 67, 021608 (2003).
- <sup>72</sup>H. Totsuji, Phys. Plasmas **8**, 1856 (2001).
- <sup>73</sup> M. Kong, A. Vagov, B. Partoens, F. M. Peeters, W. P. Ferreira, and G. A. Farias, Phys. Rev. E 70, 051807 (2004).
- <sup>74</sup> K. Nelissen, B. Partoens, and F. M. Peeters, *Phys. Rev. E* **69**, 046605 (2004).
- <sup>75</sup>Y.-J. Lai and L. I, Phys. Rev. E **64**, 015601 (2001).
- <sup>76</sup>G. A. Farias and F. M. Peeters, Solid State Commun. 100, 711 (1996).
- <sup>77</sup> J. A. Drocco, C. J. O. Reichhardt, C. Reichhardt, and B. Jankó, Phys. Rev. E 68, 060401 (2003).
- <sup>78</sup>V. M. Bedanov and F. M. Peeters, Phys. Rev. B 49, 2667 (1994).
- <sup>79</sup> W.-T. Juan, Z.-H. Huang, J.-W. Hsu, Y.-J. Lai, and L. I, Phys. Rev. E **58**, R6947
- 80 G. E. Astrakharchik, A. I. Belousov, and Y. E. Lozovik, J. Exp. Theor. Phys. 89, 696 (1999).
- <sup>81</sup>G. A. Hebner, M. E. Riley, D. S. Johnson, P. Ho, and R. J. Buss, Phys. Rev. Lett. 87, 235001 (2001).
- <sup>82</sup>M. Klindworth, A. Melzer, A. Piel, and V. A. Schweigert, Phys. Rev. B 61, 8404 (2000).
- <sup>83</sup> A. Melzer, M. Klindworth, and A. Piel, Phys. Rev. Lett. **87**, 115002 (2001).
- <sup>84</sup> A. Melzer, Phys. Rev. E **67**, 016411 (2003).
- <sup>85</sup> A. Melzer, IEEE Trans. Plasma Sci. **32**, 594 (2004).
- <sup>86</sup>K. Qiao, J. Kong, J. Carmona-Reyes, L. S. Matthews, and T. W. Hyde, Phys. Rev. E 90, 033109 (2014).
- <sup>87</sup>G. A. Hebner, M. E. Riley, and K. E. Greenberg, *Phys. Rev. E* **66**, 046407 (2002).
- <sup>88</sup>M. Wolter and A. Melzer, *Phys. Rev. E* **71**, 036414 (2005).
- <sup>89</sup> A. Schella, M. Mulsow, A. Melzer, J. Schablinski, and D. Block, Phys. Rev. E **87**, 063102 (2013).
- <sup>90</sup> A. K. Mukhopadhyay and J. Goree, Phys. Rev. Lett. 109, 165003 (2012).
- 91 A. Melzer, H. Krüger, S. Schütt, and M. Mulsow, Phys. Plasmas 27, 033704
- 92 A. Melzer, H. Krüger, S. Schütt, and M. Mulsow, Phys. Plasmas 26, 093702 (2019).

- <sup>93</sup> H. Kählert, A. Melzer, M. Puttscher, T. Ott, and M. Bonitz, Eur. Phys. J. D 72, 83 (2018).
- <sup>94</sup>M. Puttscher, A. Melzer, U. Konopka, S. LeBlanc, B. Lynch, and E. Thomas, Jr., Phys. Plasmas 24, 013701 (2017).
- <sup>95</sup>M. Puttscher and A. Melzer, Phys. Plasmas **22**, 073701 (2015).
- <sup>96</sup>M. Puttscher and A. Melzer, Phys. Plasmas **21**, 123704 (2014).
- 97 M. Puttscher and A. Melzer, New J. Phys. 16, 043026 (2014).
- <sup>98</sup> A. V. Timofeev, V. S. Nikolaev, and V. P. Semenov, J. Exp. Theor. Phys. 130, 153 (2020).
- <sup>99</sup>S. Singh, P. Bandyopadhyay, K. Kumar, and A. Sen, Phys. Plasmas 30, 043706 (2023).
- <sup>100</sup>Y.-f. Li, U. Konopka, K. Jiang, T. Shimizu, H. Höfner, H. M. Thomas, and G. E. Morfill, Appl. Phys. Lett. **94**, 081502 (2009).
- <sup>101</sup> M. K. Ivory, A. Kato, A. Hasanzadeh, and B. B. Blinov, Rev. Sci. Instrum. 91, 053201 (2020).
- <sup>102</sup>J. E. Allen, Phys. Scr. **45**, 497 (1992).

- <sup>103</sup>H. M. Mott-Smith and I. Langmuir, Phys. Rev. 28, 727 (1926).
- 104 V. Suresh, L. Li, J. R. G. Felipe, and R. Gopalakrishnan, J. Phys. D: Appl. Phys. 54, 275205 (2021).
- 105 I. H. Hutchinson, Plasma Phys. Controlled Fusion 48, 185 (2006).
- <sup>106</sup>S. A. Khrapak, A. V. Ivlev, S. K. Zhdanov, and G. E. Morfill, Phys. Plasmas 12, 042308 (2005).
- <sup>107</sup>H. Thomsen and M. Bonitz, Phys. Rev. E **91**, 043104 (2015).
- $^{108}\mathrm{F}.$  M. Peeters, B. Partoens, V. A. Schweigert, and G. Goldoni, Physica E 1, 219 (1997).
- <sup>109</sup>U. R. Kortshagen, R. M. Sankaran, R. N. Pereira, S. L. Girshick, J. J. Wu, and E. S. Aydil, Chem. Rev. 116, 11061 (2016).
- 110 D. Mariotti and R. M. Sankaran, J. Phys. D: Appl. Phys. 43, 323001 (2010).
- <sup>111</sup>T. Lafleur, J. Schulze, and Z. Donkó, Plasma Sources Sci. Technol. 28, 040201 (2019).